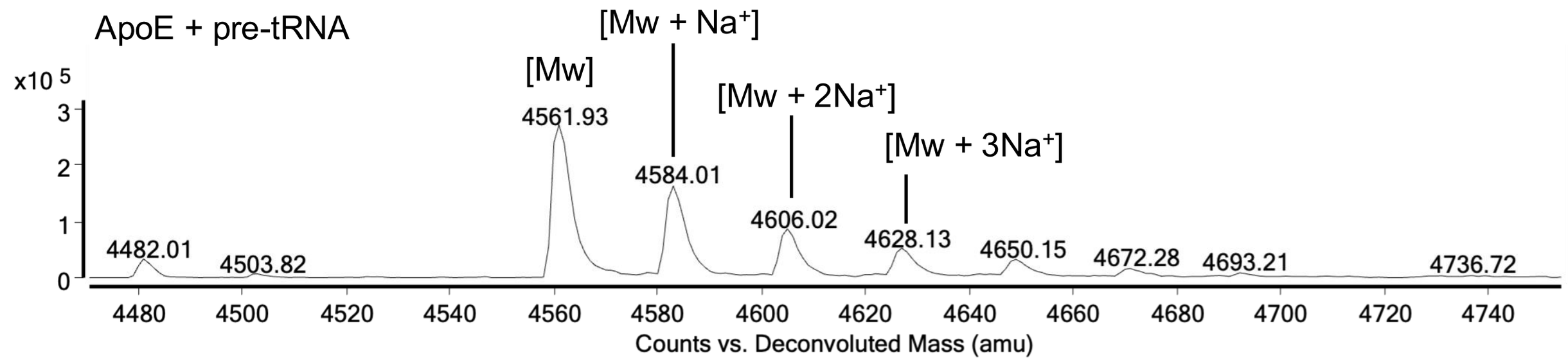

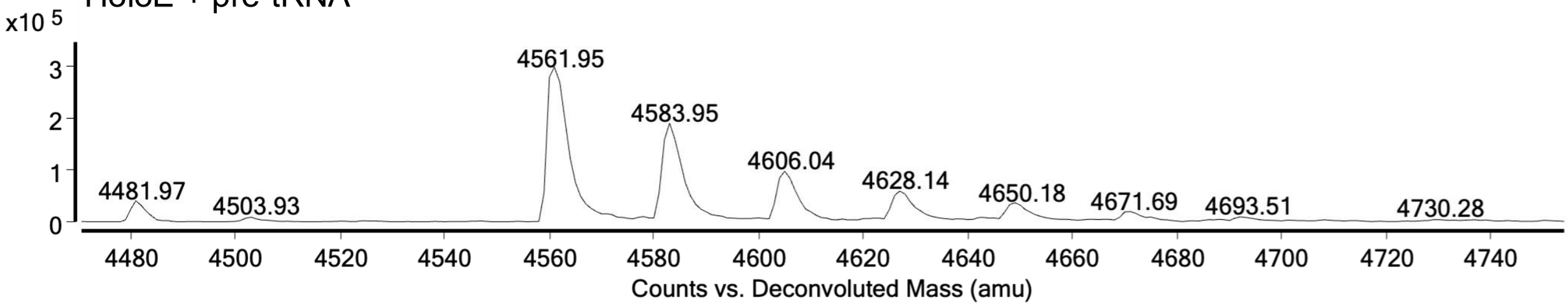

Supplementary Fig. 1 | Mass spectrometry assessment to confirm the molecular mass of the 5′-leader product of pre-tRNA, produced by RNase P apo and holoenzyme. Ionization states and deconvoluted molecular mass distributions of the 5′ cleavage product of pre-tRNA by apoE (top) and holoE (bottom).

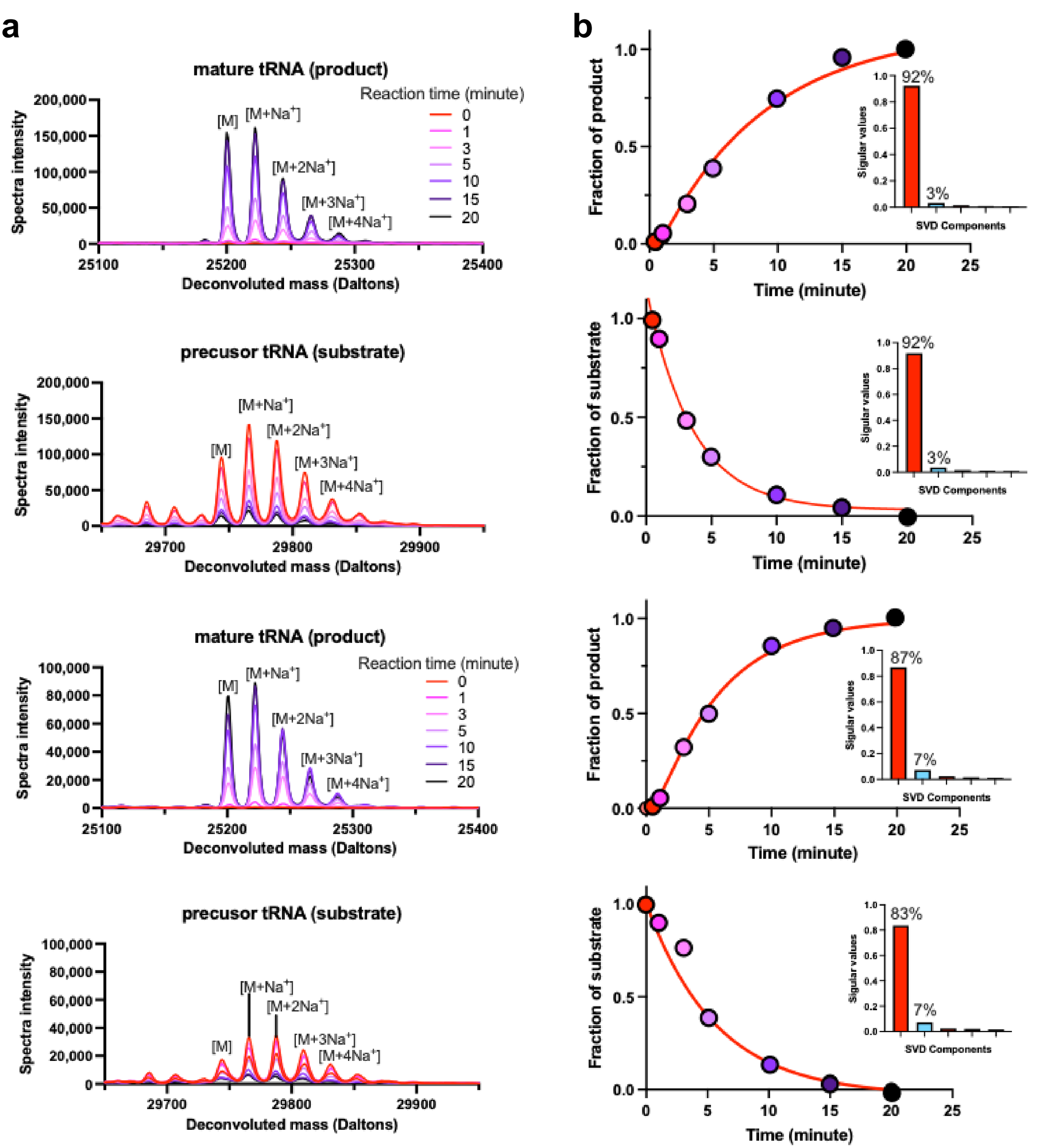

Supplementary Fig. 2 | Time-course experiments of precursor tRNA hydrolysis by RNase P holoE through quantitative mass-based analysis. a, Time-dependent mass distributions of product formation (mature tRNA) and depletion of substrate (pre-tRNA) from experimental duplicate, n=2. **b,** Fraction of product (top) and substrate (bottom) as a function of time derived from singular value decomposition (SVD) analysis of the time-course mass signals fit by the kinetic model (**Methods**).

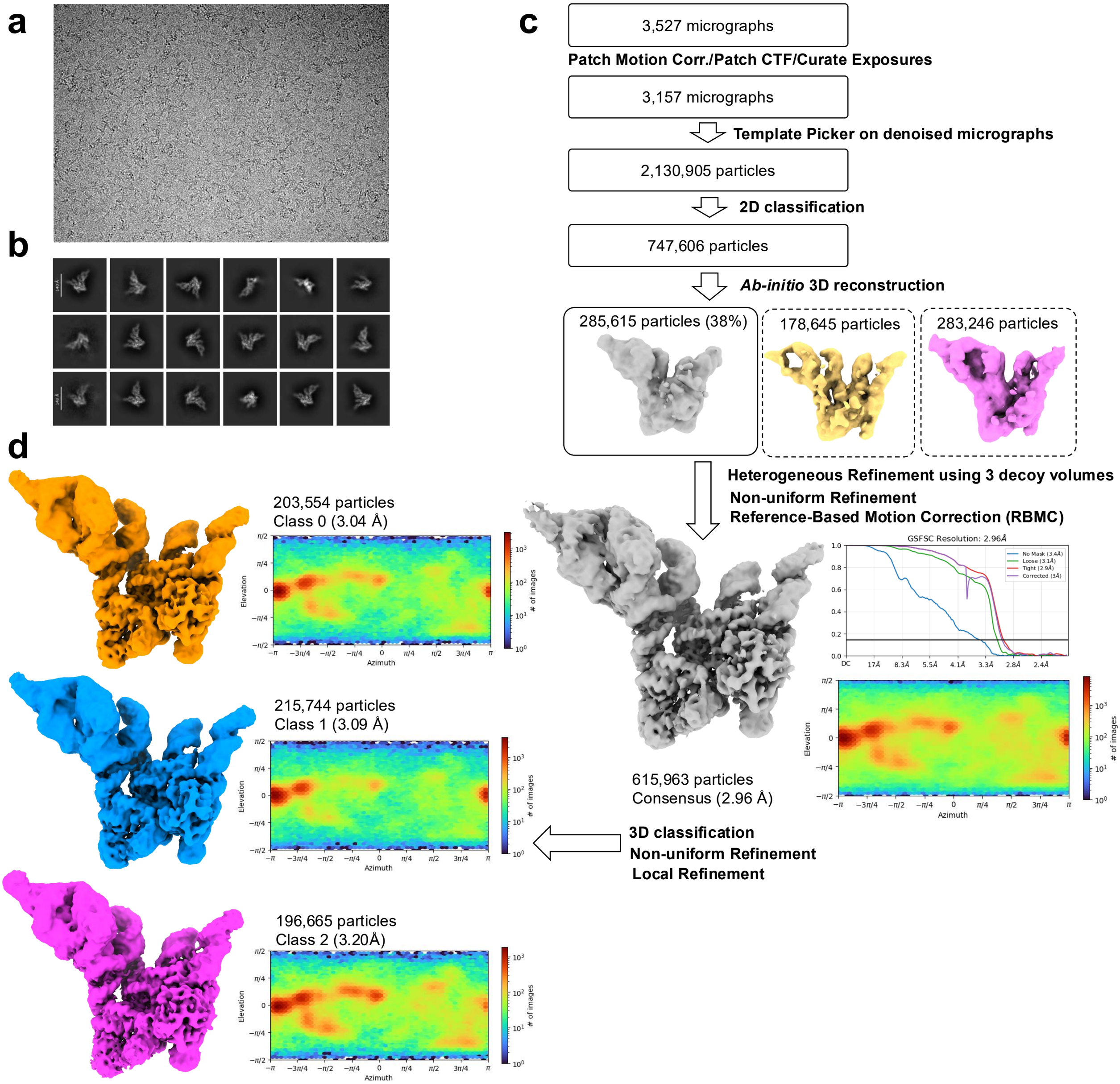

Supplementary Fig. 3 | Cryo-EM workflow and analysis of RNase P RNA holoenzyme (holoE), related to Figure S3B. (A) Representative cryo-EM micrograph after motion correction. **(B)** Representative 2D class averages of extracted particles. **(C)** CryoSPARC workflow from image processing to 3D reconstruction and refinement, including reference-based motion correction (RBMC). **(D)** The consensus volume of holoE was sub-classified into three distinct volumes. The Euler angle distribution of the particle images for the three cryo-EM maps is shown on the right.

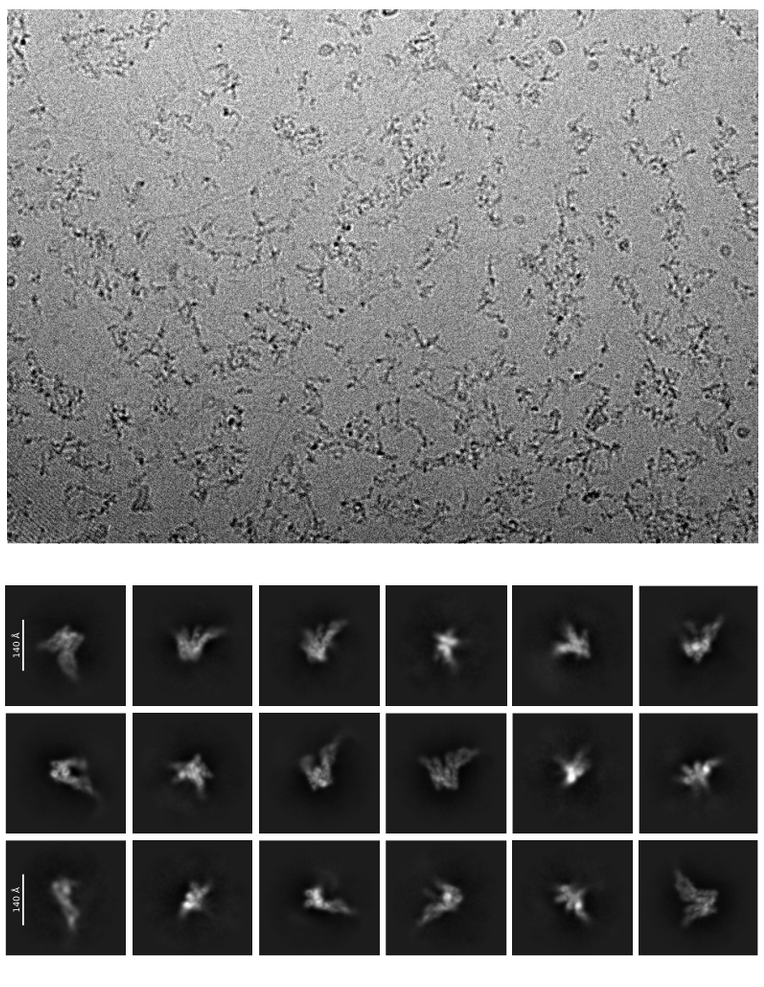

Supplementary Fig. 4 | Cryo-EM workflow and analysis of RNase P holoenzyme in complex with pre-tRNA (holoES). (A) Representative cryo-EM micrograph after motion correction. **(B)** Representative 2D class averages of extracted particles. **(C)** CryoSPARC workflow from image processing to 3D reconstruction and refinement. The consensus volume particle stack was subclassified by 3D classification using a focus mask around the tRNA to purify the particles containing substrate. (**D**) The purified stack of holoES particles was polished by reference-based motion correction (RBMC), followed by non-uniform and local refinement. Euler angle distribution of the particle images for the cryo-EM map is shown at the bottom.

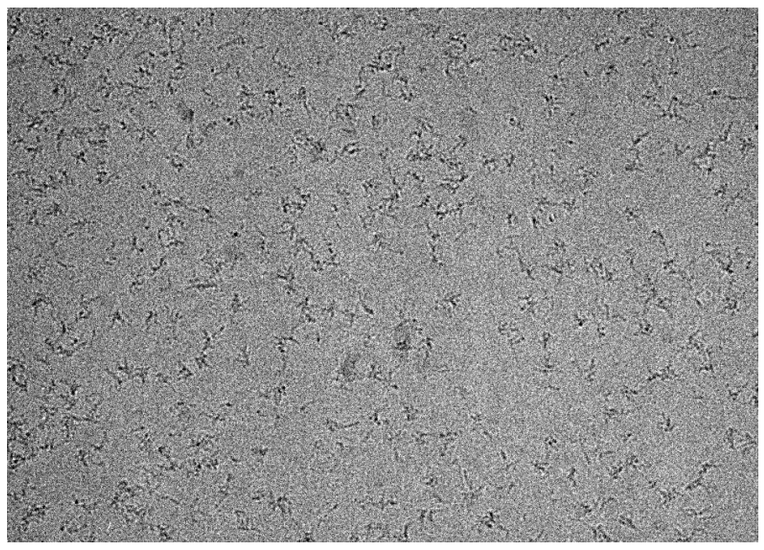

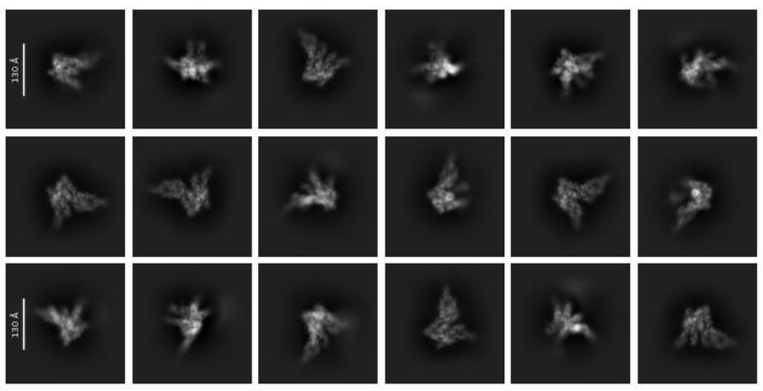

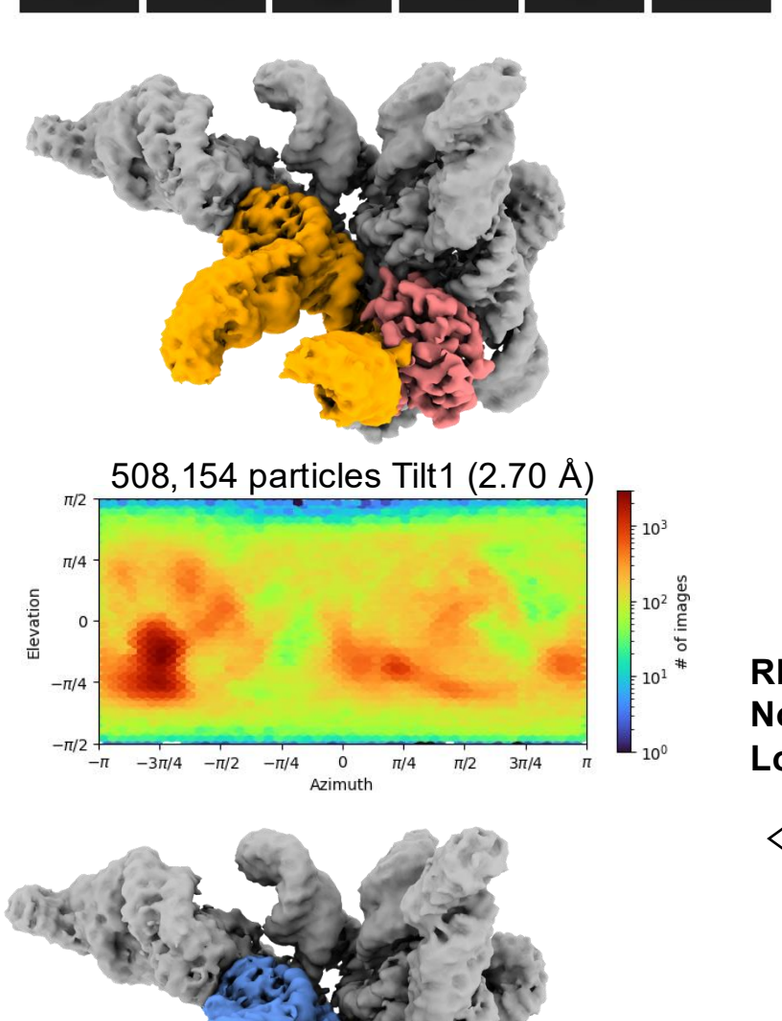

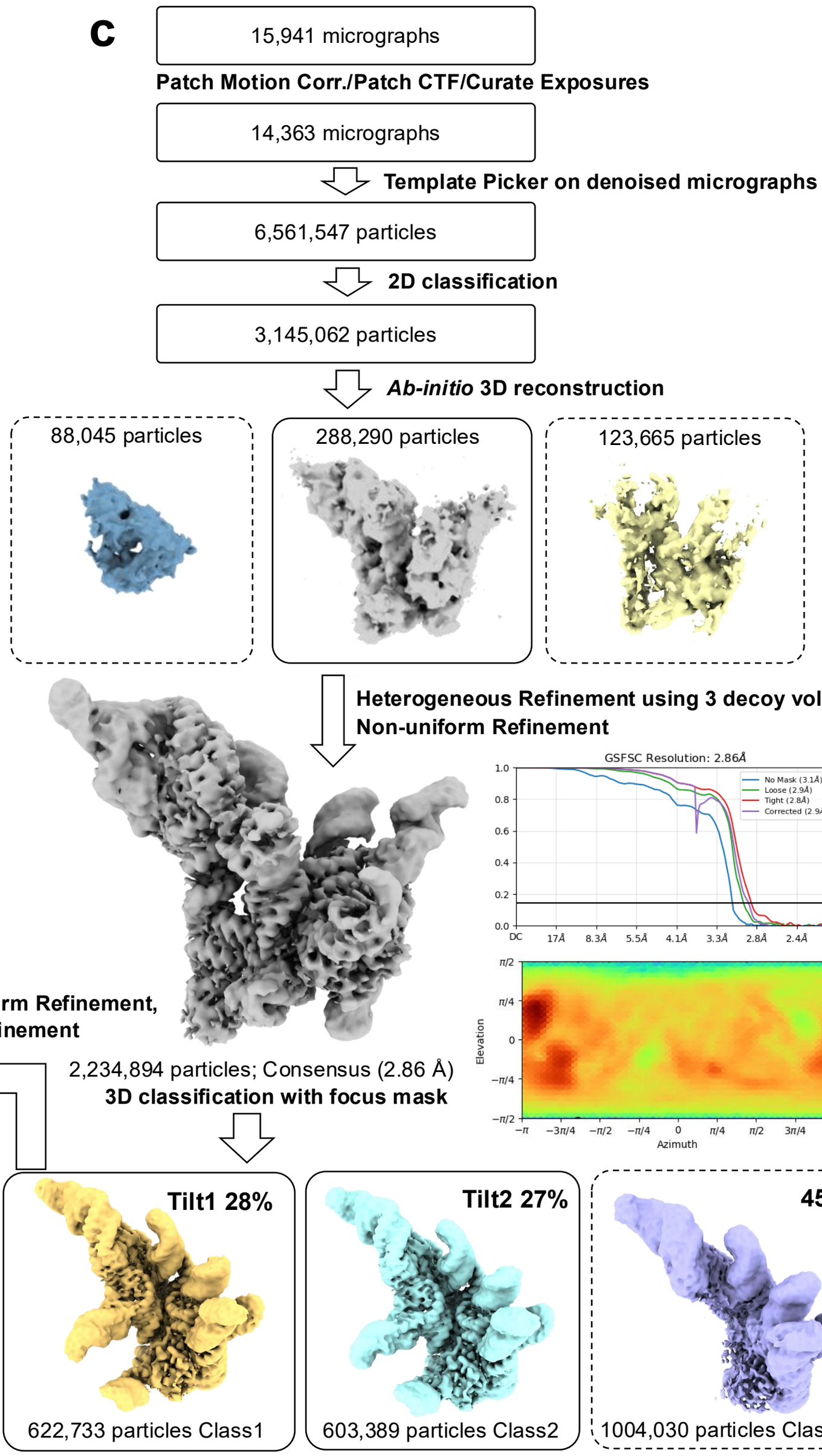

Supplementary Fig. 5 | Cryo-EM workflow and analysis of RNase P holoenzyme in complex with loop-back (LB) pre-tRNA. (A) Representative cryo-EM micrograph after motion correction. **(B)** Representative 2D class averages of extracted particles. **(C)** CryoSPARC workflow from image processing to 3D reconstruction and refinement. The consensus volume particle stack was subclassified by 3D classification using a focus mask around the tRNA to purify the particles containing substrate, which resulted in the two volumes with different tRNA tilt angles (**D**) The purified stacks of particles were polished by reference-based motion correction (RBMC), followed by non-uniform and local refinement. Euler angle distribution of the particle stacks for the two cryo-EM maps of holoES-LB-pre-tRNA is shown at the bottom.

a

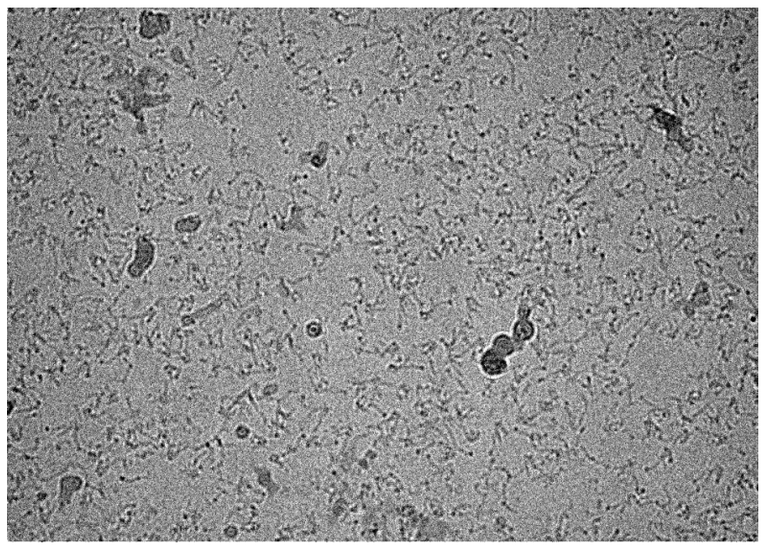

b

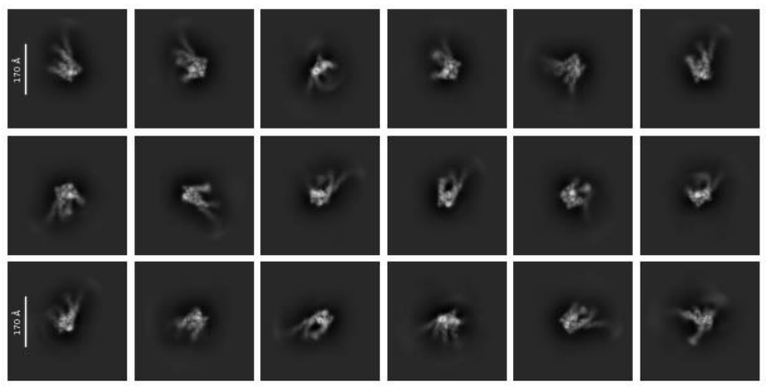

c

15,041 micrographs

Patch Motion Corr./Patch CTF/Curate Exposures/Denoise

14,442 micrographs

Template Picker on denoised micrographs

3,990,689 particles

2D classification

2,873,107 particles

***Ab-initio* 3D reconstruction**

2,220,360 particles

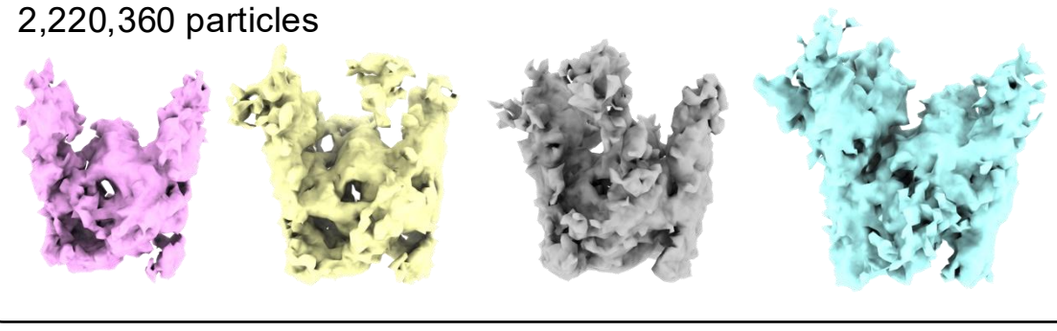

Heterogeneous Refinement using 3 decoy volumes
Non-uniform Refinement
3D classification

d

Sub-class1-1 (2.96 Å) **:** 157,466 particles

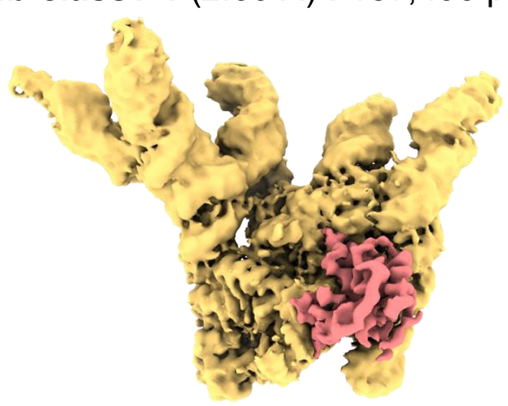

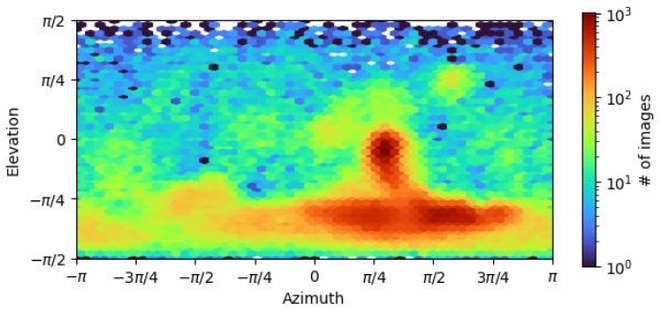

Sub-class1-2 (3.02 Å**):** 133,224 particles

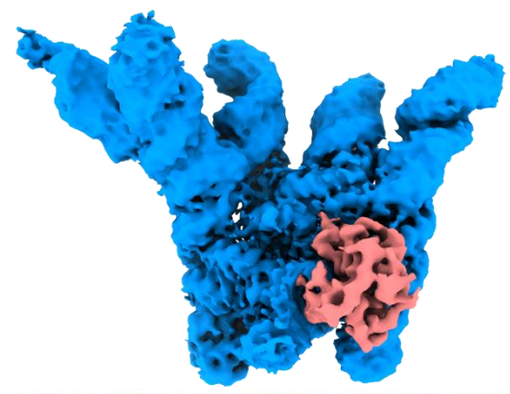

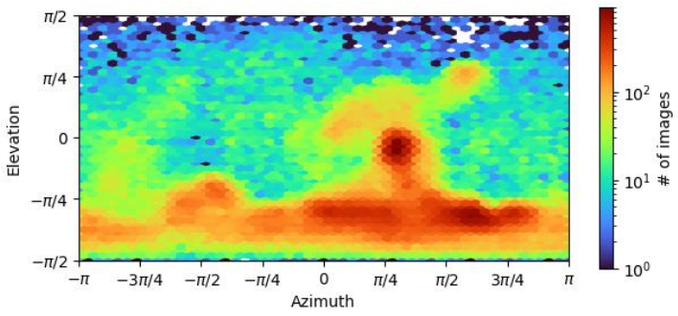

3D classification

RBMC,
Non-uniform &
Local Refinement

Class1 (26%): 571,270 particles

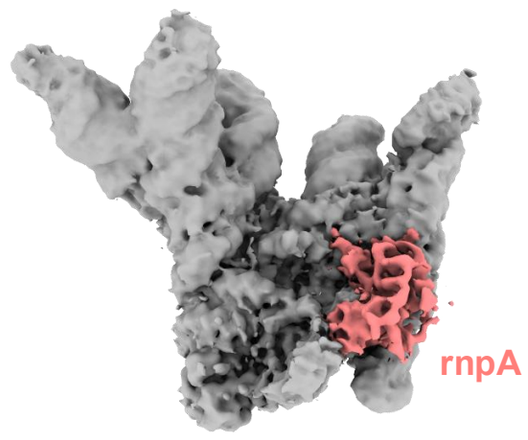

HoloE-TLm

Class2 (14%): 309,996 particles

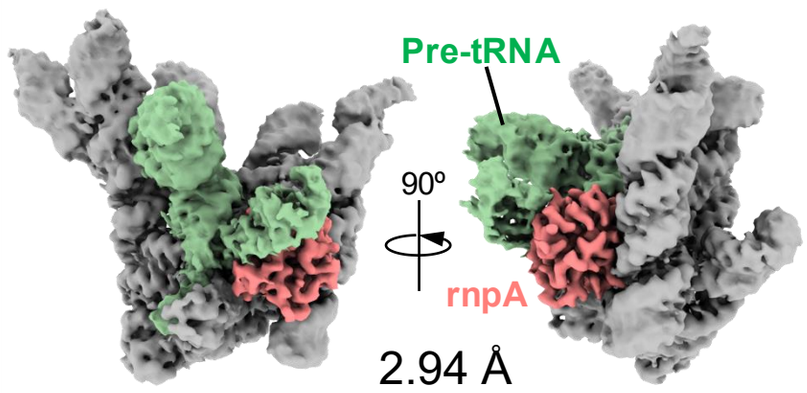

2.94 Å

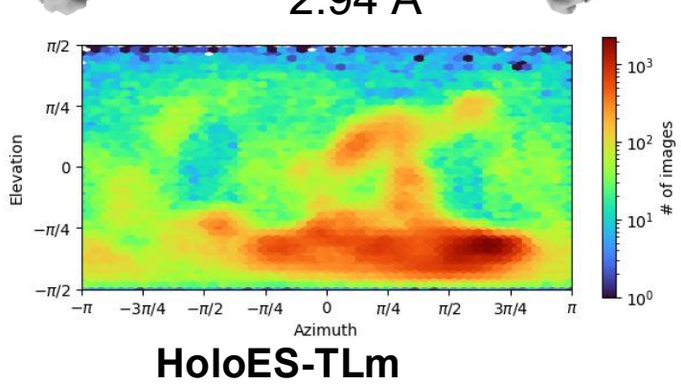

HoloES-TLm

Class0 (22%): 493,155 particles

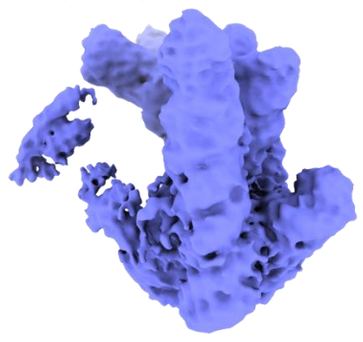

HoloES-TLm

Class3 (17%): 384,583 particles

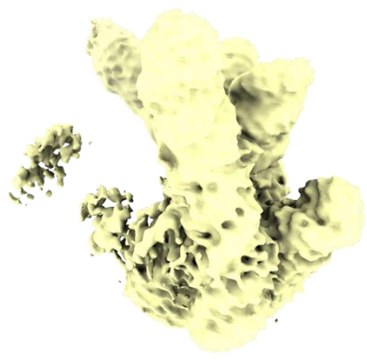

HoloES-TLm

Class4 (21%): 451,211 particles

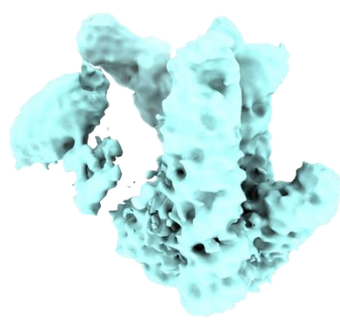

HoloES-TLm

Supplementary Fig. 6 | Cryo-EM workflow and analysis of RNase P tetraloop mutant holoenzyme (TLm-holoE) and its complex with pre-tRNA (TLm-holoES). (A) Representative cryo-EM micrograph after motion correction. **(B)** Representative 2D class averages of extracted particles. (**C)** CryoSPARC workflow from image processing to 3D reconstruction and refinement. The consensus volume particle stack was subclassified by 3D classification into five distinct sub-volumes. Three of these volumes (Classes 0, 3, and 4) showed partial density for pre-tRNA in a location different from the catalytic position. One volume (Class 2) showed the complete ternary complex (holoES-TLm), and one volume (Class 1) showed no bound substrate (holoE-TLm). (**D**) The holoE-TLm volume was further classified into two sub-volumes based on the differences in the S-domain. The final volumes of holoE-TLm and holoES-TLm were polished by reference-based motion correction (RBMC), followed by non-uniform and local refinement. Euler angle distribution of the particle images for the three cryo-EM maps is shown at the bottom.